# The ACUSITT Ultrasonic Ablator: The First Steerable Needle with an Integrated Interventional Tool

E. Clif Burdette[1], D. Caleb Rucker[4], Punit Prakash[3], Chris J. Diederich[3], Jordan M. Croom[4], Clyde Clarke[2], Philipp Stolka[2], Titania Juang[3], Emad M. Boctor[2], and Robert J. Webster III[4*]

[1]Acoustic MedSystems, Inc., Champaign, IL USA
[2] Department of Radiology, Johns Hopkins University, Baltimore, MD USA
[3]Department of Radiation Oncology, University of California, San Francisco, CA USA
[4]Department of Mechanical Engineering, Vanderbilt University, Nashville, TN USA

## ABSTRACT

Steerability in percutaneous medical devices is highly desirable, enabling a needle or needle-like instrument to avoid sensitive structures (e.g. nerves or blood vessels), access obstructed anatomical targets, and compensate for the inevitable errors induced by registration accuracy thresholds and tissue deformation during insertion. Thus, mechanisms for needle steering have been of great interest in the engineering community in the past few years, and several have been proposed. While many interventional applications have been hypothesized for steerable needles (essentially anything deliverable via a regular needle), none have yet been demonstrated as far as the authors are aware. Instead, prior studies have focused on model validation, control, and accuracy assessment. In this paper, we present the first integrated steerable needle-interventional device. The ACUSITT integrates a multi-tube steerable Active Cannula (AC) with an Ultrasonic Interstitial Thermal Therapy ablator (USITT) to create a steerable percutaneous device that can deliver a spatially and temporally controllable (both mechanically and electronically) thermal dose profile. We present our initial experiments toward applying the ACUSITT to treat large liver tumors through a single entry point. This involves repositioning the ablator tip to several different locations, without withdrawing it from the liver capsule, under 3D Ultrasound image guidance. In our experiments, the ACUSITT was deployed to three positions, each 2cm apart in a conical pattern to demonstrate the feasibility of ablating large liver tumors 7cm in diameter without multiple parenchyma punctures.

**Keywords:** Ultrasound, Steerable Needle, Robot, Liver, Image-Guided Surgery, Image-Guided Therapy, Ablation

## 1. INTRODUCTION

Needle-based procedures are pervasive in medicine, because needles are among the least invasive vehicles for accessing the interior of the human body. Needles can be used for diagnoses (e.g. biopsy), as well as interventions (e.g. injection of liquid therapeutic agents, radioactive seed implantation, thermal therapy, etc.). Accuracy in targeting the desired location is essential in nearly all needle-based procedures to ensure therapeutic or diagnostic efficacy and safety. It has been well-established that image-guided robotic devices are useful for aligning needles accurately with preoperatively planned insertion trajectories. For example, a single robotic insertion has been shown to exhibit approximately half the error of a manual insertion by an experienced surgeon under Ultrasound guidance [Boctor-2008].

However, initial robotic alignment of the needle toward its target can never completely eliminate tip placement error, because there is no means of compensation for registration error (which can never be completely eliminated) or perturbations that occur during insertion, including tissue deformation, patient motion, breathing, deflection of the needle at membrane boundaries, etc. Furthermore, there are some locations that are inaccessible to straight-line trajectories (e.g. the pubic arch can obstruct a portion of the prostate in some patients during brachytherapy). These factors have motivated the recent development of steerable needles, and many mechanisms for steering have been proposed. To date, all steerable needle research has focused on tip placement accuracy assessment and model validation, which are necessary first steps toward interventional and diagnostic goals.

*robert.webster@vanderbilt.edu phone 1 615 322-0193; fax 1 615 343-6687; http://research.vuse.vanderbilt.edu/MEDLab/

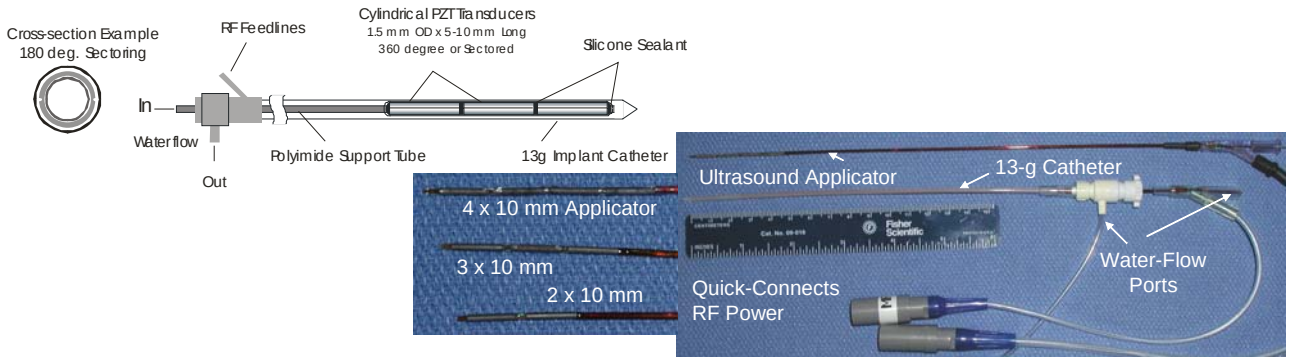


**Figure 1.** Ultrasound Interstitial Thermal Therapy (USITT) flexible interstitial ultrasound applicators designed for heating from within catheters, recirculating water to cool elements and provide acoustic coupling. Separate control of multiple transducer sections, ability to sector and angularly direct energy, and favorable energy penetration make this the most controllable, conformable interstitial heating technology.

In this paper, we present what we believe to be the first integrated steerable needle/interventional tool, an Ultrasonic Interstitial Thermal Therapy probe (USITT) [Diederich-1996a, Diederich-1999, Nau-2001] (See Figure 1) integrated with an Active Cannula (AC) [Webster-2009] (See Figure 2). We also present our initial ex vivo experimental results in applying the integrated ACUSITT device to the challenging task of ablating a large volume of liver tissue through a single entry point in the liver parenchyma. Since the ACUSITT enables both mechanical and electrical steering of thermal treatment, it can ablate large and/or geometrically complex volumes of tissue through a single insertion. We envision the ACUSITT working in conjunction with 3D Ultrasound [Boctor-2009] to enable accurate ablative treatment, real-time temperature monitoring and control, and thermal dose validation in large and/or geometrically complex ablation tasks in many areas of the body.

### 1.1 Related Work on Steerable Needles

The state of the art in steerable needles has been summarized in the recent MICCAI needle steering workshop [MICCAI-2008], and further references can be found in [Webster-2007]. A number of mechanisms for steering have been demonstrated, including applying base angulations and lateral forces to stiff traditional needles with symmetric tips [DiMaio-2003, Glozman-2007], steering semi-flexible needles using a pre-bent stylet inside a straight cannula [Okazawa-2005], and steering highly flexible needles by harnessing asymmetric bevel tip forces [Webster-2006a]. An alternate technique that can be less dependent on tissue properties uses multiple precurved concentric cannulae, which are gripped at their respective bases and actuated by axial rotation and telescopic translation of each individual tube [Webster-2006b, Dupont-2006, Terayama-2007, Webster-2009, Rucker-2009]. This design, sometimes called an Active Cannula, uses tube elastic interaction to change its shape, and thus can "steer" through free space as well as soft tissues. The Active Cannula tubes can also be designed to be stiff relative to the tissue, making cannula trajectory less dependent on tissue properties than methods like bevel steering that make use of the needle-tissue interaction forces to steer. The current status of all of these methods of steering is proof of concept – none have yet been used for sample collection or therapy delivery, as far as the authors are aware.

**Figure 2**. A prototype 4-tube Active Cannula (AC), made from precurved superelastic tubes, which changes shape as tubes are extended and rotated relative to one another. The USITT shown in Figure 1 was integrated with the AC to create the ACUSITT steerable acoustic ablator – the first steerable needle with an integrated interventional tool of which the authors are aware.

### 1.2 Medical Motivation for Liver Ablation

Hepatocellular carcinoma is the most common type of primary liver cancer with over one million new cases worldwide per year [Kim-2005]. Metastatic disease from other sites is also frequent. For example, 146,000 new cases of colorectal cancer were diagnosed in the USA in 2005 and 50% of these (73,000 patients) developed liver metastases. Many recent studies have demonstrated the efficacy of interstitial ablative approaches for the treatment of hepatic tumors using RF ablation [Choti-2002] and other techniques. Despite these promising results, current systems remain highly dependent on operator skill, and cannot treat many tumors because there is insufficient control of the size and shape of the zone of necrosis, and no control over ablator trajectory within tissue, both of which our ACUSITT is designed to address.

### 1.3 Ultrasonic Interstitial Ablation Technology

Localized heating of tissue with ultrasound interstitial thermal therapy (USITT) applicators is caused by mechanical losses from the propagation of the acoustic waves through the tissue. The longitudinal pressure waves travel through the tissue and apply mechanical force on the tissue, producing oscillatory motion that generates frictional heat, which coagulates tissue. The nature of the coagulation produced is solid and consistent throughout the lesion, without regions of charring or vaporization, as are commonly produced using other techniques such as RF or laser ablation. Further discussion on this topic can be found in [Diederich-2004, Nau-2001].

## 2. METHODS

### 2.1 The ACUSITT Device

The USITT (see Figure 1) consists of interstitial ultrasound applicators that utilize arrays of small tubular ultrasound radiators designed to be inserted within plastic implant catheters. The applicators are fabricated with multiple tubular segments, with separate power control, so that the power deposition pattern can be adjusted in real time along the applicator axis. The ultrasound energy emanating from each transducer section is highly collimated within the borders of each segment so that the axial length of the therapeutic temperature zone is well defined by the number of active elements and applied power levels. Angular or rotational heating patterns can be modified by sectoring the transducer surface. In this fashion, active zones can be selected (i.e., 90°, 180°, or 360°) to produce angularly selective heating patterns. Applicators are tested for electrical and acoustic benchmark performance, followed by evaluation of thermal performance with *in-vitro* and *in-vivo* animal studies.

Figure 3 shows the USITT within an Active Cannula (AC). An AC consists of several concentric precurved elastic tubes. The AC changes shape as these tubes axially extend and rotate, when actuated at their bases. Figure 2 shows a photo of a 4-tube AC, while Figure 3 (Left) shows the manual actuation unit used in our experiments in this paper. Integrating the AC and USITT is conceptually simple. Since the USITT is flexible, it can be delivered through the central working channel of an AC with appropriately sized tubes. The experimental prototype and actuation mechanism used in our experiments described in this paper are shown in Figure 3.

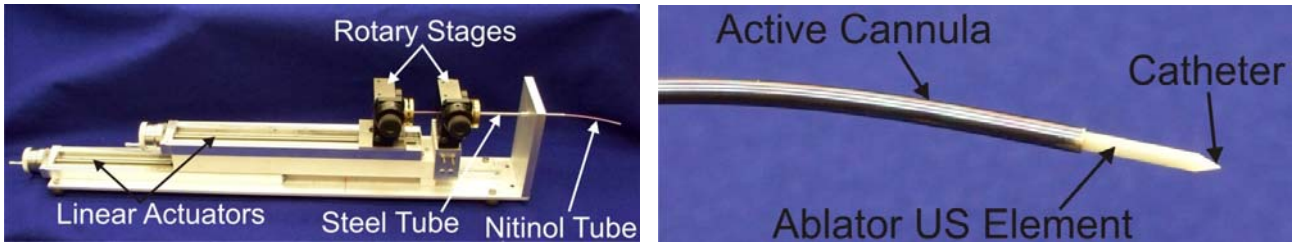


**Figure 3**. (Left) Our experimental apparatus consists of manual insertion and rotation stages for a two-tube AC. (Right) Photo of an ACUSITT tip showing the USITT delivered through an AC.

### 2.2 Experimental Testbed

In the experiments described in Section 3, we used the experimental setup pictured in Figure 4(Left). It consists of a Cartesian robot that manipulates an Ultrasound probe, a container that holds ex vivo bovine liver encased in gelatin, the manual AC actuation unit described above, and the ACUSITT device it delivers. During experiments, the manual AC actuation unit is slid forward, such that the plate on the front of the actuation unit is flush with the surface of the tissue container.

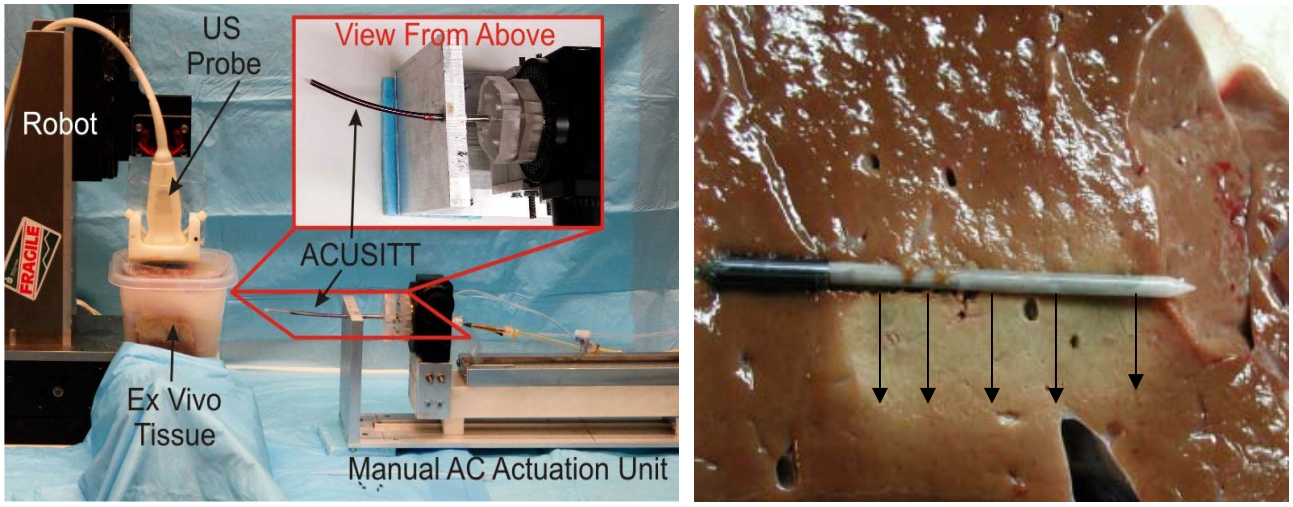


**Figure 4**. (Left) Experimental apparatus for ex vivo ablation experiments monitored via ultrasound imaging. (Right) Ablation experiment showing the directional capability of the USITT.

### 2.3 *Ex-Vivo* Animal Tissue Experiments

Bovine livers were acquired immediately after slaughter for use in these experiments. Large sections (one or two lobes) were removed and degassed in saline. The degassed specimens were placed within circulating 37C saline and allowed to come to temperature equilibrium. Thermal lesions were produced with single USITT applicator placement with three independent transducers on a single applicator (electronic control of active ablator length), with either 360 degree or 180 degree angular directivity. Once in position, the USITT catheter was inserted within the liver tissue along the determined trajectory and an ablation performed. This process was repeated for a total of three sequential ablations. Lesions were performed for either 10 or 15 min power on sequences. Experimental results are given in Section 5 below.

## 3. ACTIVE CANNULA KINEMATIC PLANNING RESULTS

As briefly described in Section 2.1, while ACs may in general have many component tubes, our particular prototype used in this work consists of two concentric elastic tubes. When the bases of these tubes are axially extended and rotated, the AC changes shape, and in this way the position of the tip can be controlled in free space. When using the AC inside tissue, it is possible to plan a specific series of base rotations and translations that will achieve a desired needle trajectory through the tissue to a desired final tip location. The central channel of the inner tube provides a means to insert the USITT into the tissue at the tip of the AC. In the prototype used in our experiments the inner tube is curved in a circular arc and is made of Nitinol, while the outer tube is straight and is made of steel to minimize its bending while in tissue (although this bending is accounted for in the model below). The circular shape of the nitinol tube was set into the material by heat treatment, and we measured the radius of curvature of the tube after this process to be 143.7mm.

One can describe the kinematics of this device (a special case of the more general models provided in [Webster-2009, Rucker-2009], which can account for an arbitrary number of component tubes with curvatures that are not restricted to circular shapes) by considering that there are three main segments or links that provide the mapping from base to tip. They are, (1) the segment where the outer tube, inner tube, and USITT are all combined (the section labeled $l_1$ in Figure 5, which is the first section inside the tissue – curvature exaggerated for illustrative purposes in the figure),

(2) the segment labeled $l_2$ where only the curved inner tube and the USITT are combined, and (3) the final straight segment where the USITT extends straight from the tip of the inner tube (this is also the area surrounded by semitransparent cylinders in Figure 6). For a given set of translations and rotations at the base of the AC, the position of the tip of the USITT can be calculated as follows.

First, we calculate the curvatures and lengths of each section,

$$
\begin{aligned}
k_1 &= \frac{E_2 I_2}{E_1 I_1 + E_2 I_2} k_2 \\
l_1 &= L_1 - D_1 \\
l_2 &= L_2 - D_2 - l_1 \\
l_3 &= L_3 - D_3 - l_1 - l_2
\end{aligned}
$$

where $I_i$ and $E_i$ are respectively the cross sectional moment of inertia and Young's Modulus of tube $i$, $k_2$ is the known curvature of the inner tube (also the curvature of the second segment) and $k_1$ is the curvature of the first segment (it will be much less than $k_2$ because the outer tube is straight and much stiffer than and the curved inner tube). The segment lengths $l_1$, $l_2$, and $l_3$ are combinations of the total lengths of each component ($L_1$, $L_2$, and $L_3$) and the translational distances between their bases and the world frame origin at the front plate of the actuation unit ($D_1$, $D_2$, and $D_3$). The Cartesian location of the tip of the USITT when the AC is in this configuration is given by,

$$
\begin{aligned}
x =& \frac{1}{k_1 k_2} \left(k_1 \cos(l_1 k_1 + l_2 k_2) - k_2 - l_3 k_1 k_2 \sin(l_1 k_1 + l_2 k_2) + (k_2 - k_2) \cos(l_1 k_1)\right) \cos(\theta) \\
y =& \frac{1}{k_1 k_2} \left(k_1 \cos(l_1 k_1 + l_2 k_2) - k_2 - l_3 k_1 k_2 \sin(l_1 k_1 + l_2 k_2) + (k_2 - k_1) \cos(l_1 k_1)\right) \sin(\theta) \\
z =& \frac{1}{k_1 k_2} \left(k_1 \sin(l_1 k_1 + l_2 k_2) + l_3 k_1 k_2 \cos(l_1 k_1 + l_2 k_2) + (k_2 - k_1) \sin(l_1 k_1)\right)
\end{aligned}
$$

where $\theta$ is the angle of axial rotation of the inner tube. The kinematic planning problem is to find the appropriate actuation inputs $D_1$, $D_2$, and $\theta$ given 1) a desired tip location for the USITT and 2) a required exposed length of the USITT for ablation, $l_3$. To accomplish this, we solve the above nonlinear system numerically using Matlab's **fsolve** function.

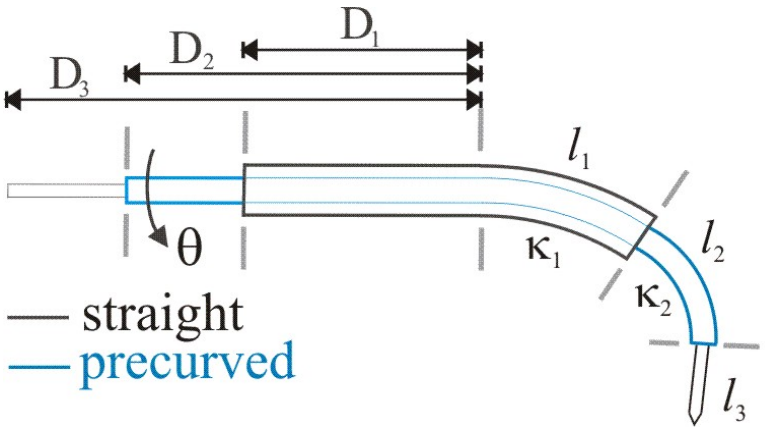


**Figure 5.** Diagram illustrating the dimensions of the ACUSITT. The USITT extends beyond the innermost active cannula tube, and is represented by the straight, pointed cylinder at the right hand side of the diagram. The USITT proceeds a fixed straight distance beyond the tip of the innermost tube, which is defined by the insertion distance necessary to extend the active elements of the USITT beyond the tip of the innermost active cannula tube.

Once the actuation inputs are obtained, the sequence for deploying the device is intuitive. First, the inner tube is rotated to the desired angle. Then both tubes and the USITT are advanced together with their tips coincident until the base of the outer tube reaches $D_1$. Then the inner tube and USITT advance together until the base of the inner tube reaches $D_2$. Lastly, the USITT advanced further, a distance of $l_3$.

The inner tube and USITT can then be retracted back inside the outer tube, rotated, and redeployed to a different location without the need to remove the outer tube from its single puncture into the liver capsule. As shown in Figure 6, this capability means that the ACUSITT is able to ablate many successive locations through a single entry point, allowing effective treatment of even large and/or geometrically complex tumors. An additional level of control is also provided by the USITT's directionality, which enables further electronic shaping of the ablation region. In section 5 we describe experimental results illustrating this capability in bovine liver tissue, and simultaneously demonstrating the accuracy of the kinematic model given here.

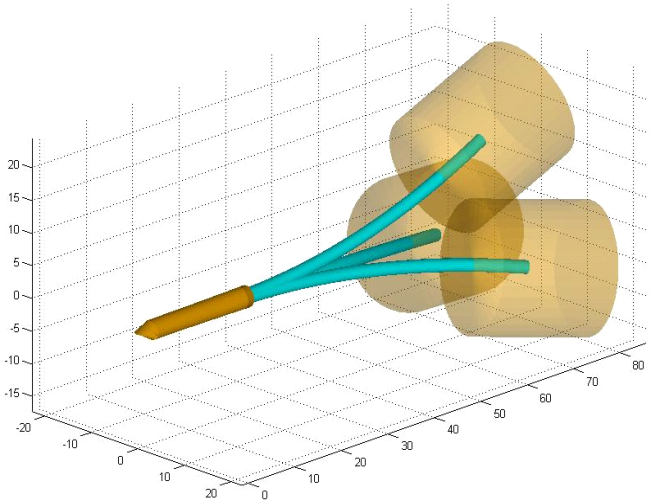


**Figure 6.** An example of a spatial plan for three successive cylindrical ablations generated by ACUSITT planning software described in this section. To deploy to one of these configurations, both tubes and the USITT are first inserted into the tissue together, with their tips coincident. Then the inner curved tube is advanced and follows a curved trajectory. Finally the USITT is deployed until its active elements are beyond the tip of the inner tube. After ablation (represented by the semitransparent cylinders), the curved tube and USITT can be retracted into the outer tube, axially rotated, and then redeployed to subsequent locations. Shown above are three (superimposed) deployments of the ACUSITT, with identical insertion distances, differing from one another by 120 degree inner tube rotation angles.

## 4. THERMAL PLANNING RESULTS

We have developed a coupled bioacoustic-thermal modeling platform using the finite element method for computing the 3D temperature and thermal dose profile in tissue after ablation with USITT applicators [Khalil-Bustany-1998, Diederich-2000, Tyreus-2002, Prakash-2009, Schutt 2008]. Our model computes the acoustic power deposition profile and then solves the Pennes bioheat equation to determine the transient temperature distribution and thermal dose profile. Dynamic changes in tissue properties (acoustic attenuation and absorption, blood perfusion and thermal conductivity) during heating are included [Dewey-1994, Damianou-1995, Tyreus-2004, Ross-2005]. Mathematical optimization algorithms can be used in conjunction with our model to determine optimal applicator positioning, power levels and treatment times, to ensure complete thermal coverage of the target volume, while sparing adjacent healthy tissue. Figure 7 shows an example temperature profile, simulating sequential ablation with three USITT applicators spaced 2.5 cm apart.

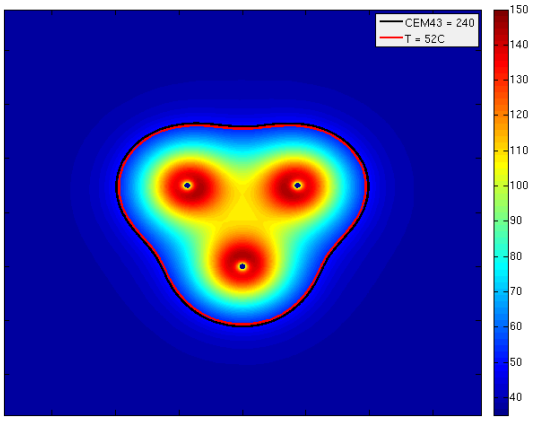


**Figure 7.** Computed temperature profile for 15 min sequential ablation with three USITT Applicators spaced 2.5 cm apart. Critical temperature and thermal dose thresholds (outline) indicate predicted boundaries of the ablation zone.

## 5. EXPERIMENTAL RESULTS

Experiments were performed with the ACUSITT combined with thermal modeling. Lesion sizes were evaluated both individually and in groups of three (lesions were created in a similar spatial pattern to that shown in Figures 6 and 7). The measurements for each single insertion trial are shown in Table 1. The A-trial measurements used a USITT applicator that radiates energy cylindrically about the ablator (active elements cover the full 360deg of the USITT shaft) and the B-trial measurements used a USITT applicator that radiates energy in a half-cylinder (active elements cover 180deg of the USITT shaft), enabling directional power delivery from the USITT tip.

Table 1. Individual insertion ablated lesion sizes.

| Trial # | Applicator | Power (W) | Time(min) | Lesion Diameter(mm) | Length (mm) |
|---|---|---|---|---|---|
| A1 | LA4.360.1 | 13 | 10 | 30 | 35 |
| 2 | LA4.360.1 | 13 | 10 | 37 | 38 |
| 3 | LA4.360.1 | 13 | 10 | 30 | 35 |
| 4 | LA4.360.1 | 13 | 15 | 45 | 40 |
| 5 | LA4.360.1 | 13 | 15 | 40 | 38 |
| 6 | LA4.360.1 | 13 | 15 | 47 | 45 |
| B1 | LA3.180.1 | 12 | 15 | 20 | 40 |
| 2 | LA3.180.1 | 12 | 15 | 20 | 38 |
| 3 | LA3.180.1 | 12 | 15 | 19 | 40 |
| 4 | LA3.180.1 | 12 | 15 | 20 | 40 |
| Trial 7-9 | 360x3 | 13 W | 10 min | 71 mm wide | 40 mm long |
| Trial 10-12 | 360x3 | 13 W | 15 min | 75 mm wide | 40 mm long |

An overall summary with averages and standard deviations is given in Table 2. For single placement and 15min treatment, average lesion diameter was 4.4cm and length was 4.1cm. For 3 placements of ACUSITT, the average ablation diameter was 7.0cm for 10min treatment and 7.5cm for 15min treatments.

Table 2. Tabulated Results Summary for Single and Multiple AC-USITT Placements.

| | Applicator | Power (W) | Time (min) | Length (mm) | Diameter (mm) |
|---|---|---|---|---|---|
| Single Applicator Placement | 3 x 360 deg. | 13 | 10 | 36.0 ± 1.7 | 32.3 ± 4.0 |
| | | 13 | 15 | 41.0 ± 3.6 | 44.0 ± 3.6 |
| | 3 x 180 deg.* | 12 | 15 | 39.5 ± 1.0 | 19.8 ± 0.5* |
| Multiple Placement | 3 x 360 deg. | 13 | 10 | 40 | 70 |
| | | | 15 | 40 | 75 |

(* Lesion radius is reported for directional 180 deg. Applicator)

The measurements given on the Tables 1 and 2 were collected as follows. After necrosing thermal dose (>300 equivalent minutes at 43C (eqm43)) within the desired target zone was achieved, ablation was ended. The specimen was sectioned and the extent of the thermal lesion observed and measured. These measurements were taken at the center of the ~2mm band where color fades from gray to red. Measured thermal dose within the treated volume ranged from 306 to 1500 eqm43 – this was measured using an array 26 gauge thermocouples inserted into the tissue. Necrosis occurs at 240 eqm43. The sectioned specimens demonstrated that a uniform ablation was obtained within the planned target zone as shown in Fig 8.

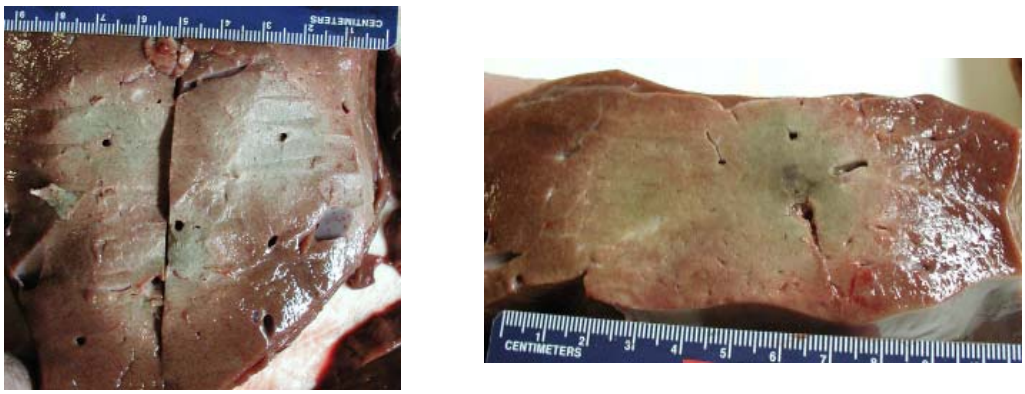


**Figure 8.** Gross pathology of an ablated bovine liver showing an ablation zone approximately 7cm across: (left) Section across treatment with three applicator positions, showing ablation lesion from three placements of a 3 x 360 deg applicator; (right) section of the lesion along the length of applicators, midplane, demonstrating a 7.5 cm wide x 4.2 cm long lesion.

We also conducted an additional experiment combining spatial planning using cannula inverse kinematics, thermal modeling, as shown in Figure 9 below. This experiment demonstrates combined spatial planning and thermal modeling, which resulted in accurate targeting of the treatment zones. The figure shows slices of ablated bovine muscle tissue for a single ACUSITT placement, dual placements spaced 2cm apart, and for a triangular placement of the ACUSITT similar to that shown in Figures 6 and 7.

**Figure 9.** Slices of Bovine muscle tissue that was ablated using the ACUSITT. These experiments were carried out using the experimental apparatus shown in Figure 4(Left), and demonstrate deployment to successive locations through a single tissue puncture point, in a spatial pattern similar to that shown in Figures 6 and 7. Slices containing one, two, and three ablations are shown.

## 6. CONCLUSION

The results presented in this paper demonstrate two novel contributions. One is the development of the first steerable needle with an integrated interventional tool, the USITT ablator, to create the ACUSITT device. The other is that this is the first system with the ability to treat a large liver tumor ablatively through a single parenchyma penetration. We intend to incorporate this device into a complete closed-loop system, where cannula positions are monitored using 3D Ultrasound images, thermal measurements are made using the Ultrasound imaging system, and elastography is used to verify ablation according to the preoperative plan. We also envision intraoperative re-planning of both subsequent spatial locations of the ACUSITT tip, as well as volumetric thermal dose shapes delivered by a directional USITT ablator.

## REFERENCES


[Boctor2008] E. M. Boctor, M. A. Choti, E. C. Burdette, and R. J. Webster III. Three-Dimensional Ultrasound-Guided Robotic Needle Placement: An Experimental Evaluation. International Journal of Medical Robotics and Computer Assisted Surgery, 4(2), 180-191, 2008.

[Boctor-2009] Boctor EM, Deshmukh N, Ayad M, Clarke C, Dickie K, Burdette E. Three-Dimensional Heat-induced Echo-Strain Imaging for Monitoring Interstitial High Intensity Ablation. The International Society for Optical Engineering (SPIE) on Medical Imaging 2009, Vol. 7265, 72650R.

[Choti2002] Choti MA, "Surgical management of hepatocellular carcinoma: resection and ablation," J Vasc Interv Radiol. 2002 Sep;13 (9 Suppl):S197-203.

[Damianou-1995] Damianou, CA, Hynynen, K, and Fan, X. Evaluation of accuracy of a theoretical model for predicting the necrosed tissue volume during focused ultrasound surgery. IEEE Transactions on Ultrasonics, Ferroelectrics, and Frequency Control, vol. 42, no. 2, pp. 182-187, 1995.

[Dewey-1994] Dewey, WC. Arrhenius relationships from the molecule and cell to the clinic. International Journal of Hyperthermia, vol. 10, no. 4, pp. 457-83, 1994.

[Diederich-1996a] Diederich, CJ. Ultrasound Applicators with Integrated Catheter-Cooling For Interstitial Hyperthermia: Theory and Preliminary Experiments. International Journal of Hyperthermia, vol. 12, no. 2, pp. 279-298, 1996.

[Diederich-1996b] Diederich CJ, Burdette EC. Transurethral ultrasound array for prostate thermal therapy: initial studies. IEEE Transactions on Ultrasonics, Ferroelectrics and Frequency Control 1996;43:1011-1022.

[Diederich-1999] Diederich, CJ, Nau, WH and Stauffer, PR. Ultrasound applicators for interstitial thermal coagulation. IEEE Transactions on Ultrasonics, Ferroelectrics, & Frequency Control, vol. 46, no. 5, pp. 1218-1228, 1999.

[Diederich-2000] Diederich, CJ, Nau, WH, Burdette, EC, Khalil Bustany, IS, Deardorff, DL and Stauffer, PR. Combination of transurethral and interstitial ultrasound applicators for high-temperature prostate thermal therapy. International Journal of Hyperthermia vol. 16, no. 5, pp. 385-403, 2000.

[Diederich-2004] Diederich CJ, Stafford RJ, Nau WH, Burdette EC, Price RE, Hazle JD. Transurethral ultrasound applicators with directional heating patterns for prostate thermal therapy: in vivo evaluation using magnetic resonance thermometry. Medical Physics. 2004 Feb;31(2):405-13.

[DiMaio-2003] DiMaio, SP and Salcudean, SE. Needle insertion modeling and simulation. IEEE Transactions on Robotics and Automation, vol. 19, no. 5, pp. 864–875, 2003.

[Glozman-2007] Glozman D and Shoham M, Image-guided robotic flexible needle steering. IEEE Transactions on Robotics, vol. 23, no. 3, pp. 459–467, 2007.

[Khalil-Bustany-1998] Khalil-Bustany IS, Diederich CJ, Polak E, Kirjner-Neto C. Minimax optimization-based inverse treatment planning for interstitial thermal therapy. International Journal of Hyperthermia, vol. 14, no. 4, pp. 347-66, 1998.

[Kim-2005] Kim WR, Gores G, Benson JT, Therneau TM, Melton LJ III,Mortality and Hospital Utilization for Hepatocellular Carcinoma in the United States , Gastroenterology, Volume 129, Issue 2, 2005, Pages 486-493.

[MICCAI-2008] http:// lcsr.jhu.edu/NeedleSteering/Workshop

[Nau-2001] Nau WH, Diederich CJ, Burdette EC. Evaluation of multielement catheter-cooled interstitial ultrasound applicators for high-temperature thermal therapy. Med Phys. 2001 Jul;28(7):1525-34.

[Okazawa-2005] Okazawa, S, Ebrahimi R, Chuang, J, Salcudean, SE and Rohling, R. Hand-held steerable needle device. IEEE/ASME Transactions on Mechatronics. vol. 10, no. 3, pp. 285–296, 2005.

[Prakash-2009] Prakash, P, Chen, X, Wootton, J, Pouliot, J, Hsu, I-C and Diederich, CJ. Patient specific optimization-based treatment planning for catheter-based ultrasound hyperthermia and thermal ablation. Proceedings of the SPIE - The International Society for Optical Engineering, vol. 7181, pp. 71810E (1-10), 2009.

[Ross-2005] Ross, AB, Diederich, CJ, Nau, WH, Tyreus, PD, Gill, H, Bouley, D, Butts, RK, Rieke, V, Daniel, B and Sommer, G. Biothermal modeling of transurethral ultrasound applicators for MR-guided prostate thermal therapy. Proceedings of the SPIE-The International Society for Optical Engineering, vol. 5698, no. 1, pp. 220-227, 2005.

[Rucker-2009] Rucker, DC, and Webster III, RJ. Parsimonious Evaluation of Concentric-Tube Continuum Robot Equilibrium Conformation. IEEE Transactions on Biomedical Engineering, 56(9), 2308-2311, 2009.

[Sears-2006] Sears, P, and Dupont, PE. A steerable needle technology using curved concentric tubes. IEEE/RSJ International Conference on Intelligent Robots and Systems, pp. 2850–2856, 2006.

[Schutt-2008] Schutt, DJ and Haemmerich, D. Effects of variation in perfusion rates and of perfusion models in computational models of radio frequency tumor ablation. Medical Physics, vol. 35, no. 8, pp. 3462-70, 2008.

[Terayama-2007] Terayama, M, Furusho, J, and Monden, M. Curved multi-tube device for path-error correction in a needle-insertion system. International Journal of Medical Robotics and Computer Assisted Surgery, vol. 3, no. 2, pp. 125–134, 2007.

[Tyreus-2002] Tyreus, PD and Diederich, CJ. Theoretical model of internally cooled interstitial ultrasound applicators for thermal therapy. Physics in Medicine and Biology, vol. 47, no. 7, pp. 1073-89, 2002.

[Tyreus-2004] Tyreus, PD and Diederich, CJ. Two-dimensional acoustic attenuation mapping of high-temperature interstitial ultrasound lesions. Physics in Medicine and Biology, vol. 49, no. 4, pp. 533-46, 2004.

[Webster-2006a] Webster III, RJ, Kim, JS, Cowan, NJ, Chirikjian, GS, and Okamura, AM. Nonholonomic modeling of needle steering. International Journal of Robotics Research, vol. 25, no. 5/6, pp. 509–526, 2006.

[Webster-2006b] Webster III, RJ, Okamura, AM, and Cowan, NJ. Toward active cannulas: Miniature snake-like surgical robots. IEEE/RSJ International Conference on Intelligent Robots and Systems, pp. 2857–2863, 2006.

[Webster-2007] R. J. Webster III. Design and Mechanics of Continuum Robots for Surgery. Ph.D. Thesis, Department of Mechanical engineering, Johns Hopkins University, Baltimore, MD, December 2007.

[Webster-2009] R. J. Webster III, J. M. Romano, and N. J. Cowan. Mechanics of Precurved-Tube Continuum Robots. IEEE Transactions on Robotics, 25(1), 67-78, 2009.